CHEMISTRY
A EUROPEAN JOURNAL

DOI: 10.1002/chem.200901976

Controlling Helical Chirality in Atrane Structures: Solvent-Dependent Chirality Sense in Hemicryptophane-Oxidovanadium(V) Complexes

Alexandre Martinez,[a] Vincent Robert,[a] Heinz Gornitzka,[b] and Jean-Pierre Dutasta*[a]

Abstract: The diastereomeric hemicryptophane oxidovanadium(V) complexes (*P*)-(*S*,*S*,*S*)-**3** and (*M*)-(*S*,*S*,*S*)-**4** have been synthesized. ^{1}H and ^{51}V NMR spectra in solution are consistent with the formation of Λ and Δ forms of the propeller-like vanatrane moiety, leading to two diastereomeric conformers for each complex: that is, (*P*)-(*S*,*S*,*S*-Λ)-**3**/(*P*)-(*S*,*S*,*S*-Δ)-**3** and (*M*)-(*S*,*S*,*S*-Λ)-**4**/(*M*)-(*S*,*S*,*S*-Δ)-**4**. The Λ/Δ ratio is rather temperature-insensitive but strongly dependent on the solvent (the *de* of (*M*)-(*S*,*S*,*S*)-**4** changes from 0 in benzene to 92% in DMSO). The solvent therefore controls the preferential clockwise or anticlockwise orientation of the propeller-like atrane unit. The energy barriers for the Λ⇄Δ equilibrium were determined by NMR experiments, and the highest $\Delta G^{\neq}$ value (103.7 kJ mol^{-1}) was obtained for (*P*)-(*S*,*S*,*S*)-**3**, much higher than those reported for other atrane derivatives. This is attributed to the constraints arising from the cage structure. Determination of the activation parameters provides evidence for a concerted, rather than a stepwise, interconversion mechanism with entropies ($\Delta S^{\neq}$) of −243 and −272 J mol^{-1} K^{-1} for (*P*)-(*S*,*S*,*S*)-**3** and (*M*)-(*S*,*S*,*S*)-**4**, respectively. The molecular structure of the (*P*)-(*S*,*S*,*S*-Λ)-**3** isomer was solved by X-ray diffraction and shows a distorted structure with one of the linkers located in the CTV cavity. Complementary quantum chemical calculations were carried out to obtain the energy-minimized structures of (*P*)-(*S*,*S*,*S*)-**3** and (*M*)-(*S*,*S*,*S*)-**4**. Our density functional theory calculations suggest that the (*P*)-(*S*,*S*,*S*-Λ)-**3** is favored, in agreement with experimental data. For the *M* series, a similar strategy was used to extract molecular structures and relative energies. As in the case of the *P* diastereomer, the Λ form dominates over the Δ one.

Keywords: chirality · hemicryptophanes · molecular structure · supramolecular chemistry · vanadium

Introduction

The use of molecular containers for the design of metalloreceptors is very attractive, because they can act as supramolecular catalysts and can mimic biological entities such as enzymes.[1] The cryptophane hosts, which are constructed from cyclotriveratrylene (CTV) units, exhibit remarkable binding properties toward neutral or charged guests[2] and are efficient in chiral recognition.[3] The related hemicryptophanes, in which dissymmetry is introduced at the molecular cavity level, are ditopic host molecules with all ingredients necessary for catalytic and recognition properties.[4,5] We have previously reported the synthesis of the diastereomeric hemicryptophanes (*P*)-(*S*,*S*,*S*)-**1** and (*M*)-(*S*,*S*,*S*)-**2** (C_3 symmetry; Scheme 1, below), which each contain a CTV unit, providing both a rigid scaffold and a lipophilic cavity. The chiral (*S*,*S*,*S*)-trialkanolamine associated with the CTV unit, with *P* or *M* configuration, gives rise to diastereomers, which were separated by chromatography.

At that time, the oxidovanadium(V) complex (*P*)-(*S*,*S*,*S*)-**3** was obtained by treatment of (*P*)-(*S*,*S*,*S*)-**1** with oxidovanadium(V) triisopropoxide.[6] The hemicryptophane-oxidovanadium(V) complex (*P*)-(*S*,*S*,*S*)-**3** includes an atrane structure, an interesting class of compounds well-represented across the periodic table and widely studied.[7] In particular, atranes, and the related azatranes, exhibit Δ or Λ stereochemistry, which generates a right- or left-handed propeller geometry, respectively (Scheme 2).[8] Interestingly, the vanadium complex provides a potential catalytic site in a chiral environment.

The Λ and Δ forms shown in Scheme 2 are closely related to the C-N-E-O dihedral angle of the five-membered rings

[a] Dr. A. Martinez, Dr. V. Robert, Dr. J.-P. Dutasta
Laboratoire de Chimie, CNRS, École Normale Supérieure de Lyon
46 Allée d'Italie, 69364 Lyon 07 (France)
Fax: (+33) 472-728-860
E-mail: jean-pierre.dutasta@ens-lyon.fr

[b] Prof. H. Gornitzka
Laboratoire de Chimie de Coordination, CNRS
205 route de Narbonne, 31077 Toulouse (France)

Supporting information for this article is available on the WWW under http://dx.doi.org/10.1002/chem.200901976.

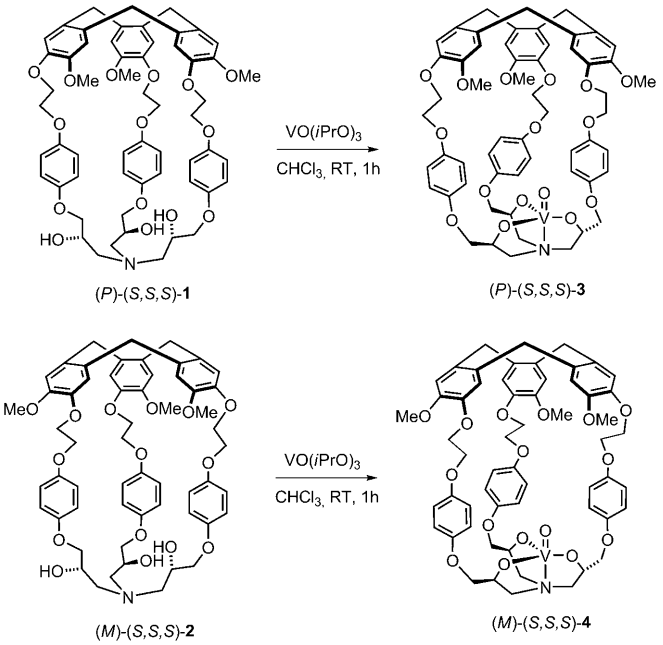

(*P*)-(*S*,*S*,*S*)-**1** (*P*)-(*S*,*S*,*S*)-**3**

(*M*)-(*S*,*S*,*S*)-**2** (*M*)-(*S*,*S*,*S*)-**4**

Scheme 1. Synthesis of diastereomers **3** and **4** from hemicryptophanes **1** and **2**, respectively.

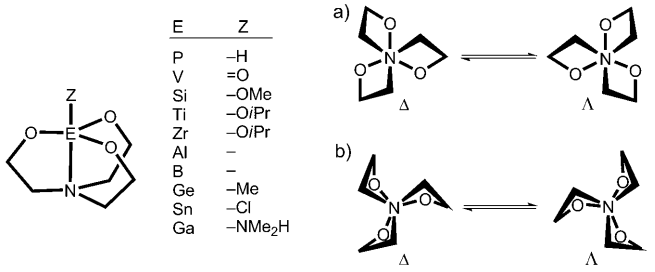

Scheme 2. Representative examples of atrane structures and their Δ and Λ forms viewed along the N–E–Z axis with N at the top. a) The substituents on the O–C carbon adopt roughly equivalent orientations; b) the substituents on the O–C carbon adopt pseudoaxial and pseudoequatorial orientations.

in the vanatrane unit.[9] In the situation depicted in Scheme 2a,[8] the substituents on the O–C carbon adopt roughly equivalent positions that do not differentiate between axial or equatorial orientations. For a dihedral angle close to 0°, the conformation of the vanatrane is better described by Scheme 2b,[9] in which the envelop conformations of the three fused five-membered rings define pseudoaxial and pseudoequatorial orientations of the O–C carbon substituents. It is common to describe the Λ and Δ forms as propeller-like arrangements, which define the helical chirality of the atrane moiety. A typical representation is shown in Scheme 2a. However, the clockwise or anticlockwise arrangements of Scheme 2b do not strictly define a helical structure. This is considered in the discussion below.

Most atrane structures are nonrigid in solution on the NMR timescale, due to rather low activation energies (typically 10 kJ mol^{-1}) for the stereoconversion of the clockwise and anticlockwise orientations of the propeller-like arrangements.[10,11] Nevertheless, some rigid structures of atrane derivatives, leading to stereoisomers sufficiently long-lived to be observed at room temperature by NMR spectroscopy, have been described in the literature. Free energies of activation of up to 74 kJ mol^{-1}, for instance, have been observed for the racemization of azaboratranes.[10] However, no attempts have been made to control the helical chirality of the atrane structure: that is, to favor the clockwise or the anticlockwise arrangement.

Here we report thermodynamic and kinetic studies of the Λ⇄Δ equilibrium for the diastereomers (*P*)-(*S*,*S*,*S*)-**3** and (*M*)-(*S*,*S*,*S*)-**4** (Scheme 1). The preferential clockwise or anticlockwise orientation of the atrane propeller, as determined from NMR and X-ray data, is examined in different solvents. The relative stabilities of the Λ and Δ forms of (*P*)-(*S*,*S*,*S*)-**3** and (*M*)-(*S*,*S*,*S*)-**4** are presented, and solvent effects are shown to affect the Λ/Δ ratio of the atrane helical conformations profoundly. Kinetic studies have demonstrated a concerted mechanism, and the activation energies obtained for these two compounds are the highest ever measured for atrane derivatives. Moreover, the solvent can control the preferential clockwise or anticlockwise orientation of the propeller-like vanatrane moiety. Density functional theory (DFT) has afforded an evaluation of the energy differences and structural data that complement X-ray and NMR experiments.

Results and Discussion

Synthesis and characterization of the complexes: The synthesis of the pure hemicryptophane diastereomer oxidovanadium(V) complex (*P*)-(*S*,*S*,*S*)-**3** (C_3 symmetry) from its precursor (*P*)-(*S*,*S*,*S*)-**1** has been reported previously.[6] The diastereomer (*M*)-(*S*,*S*,*S*)-**4** was prepared from (*M*)-(*S*,*S*,*S*)-**2** by the same experimental procedure (Scheme 1). The ^{1}H NMR spectrum of (*M*)-(*S*,*S*,*S*)-**4** presents a rather puzzling situation (Figure 1): a mixture of two compounds was observed, but several attempts to isolate them failed. Moreover, a more accurate analysis of the previously published ^{1}H NMR spectrum of (*P*)-(*S*,*S*,*S*)-**3** in $CDCl_3$ also revealed the presence of small amounts of a second compound. In neither case could these supplementary signals be attributed to the free ligand.

Rehder et al. had recently reported that a monomer/dimer equilibrium could possibly be responsible for such a ^{1}H NMR pattern in alkanolamine oxidovanadium complexes.[12] However, a similar intermolecular association to explain the NMR spectra of (*P*)-(*S*,*S*,*S*)-**3** and (*M*)-(*S*,*S*,*S*)-**4** complexes would be highly improbable because of the expected steric hindrance due to the hemicryptophane hosts. Careful 1D- and 2D-NMR analyses were therefore performed on solutions of both diastereomers (see Figures S1–S4 in the Supporting Information). In these experiments, each diastereomer gave ^{1}H NMR spectra containing two

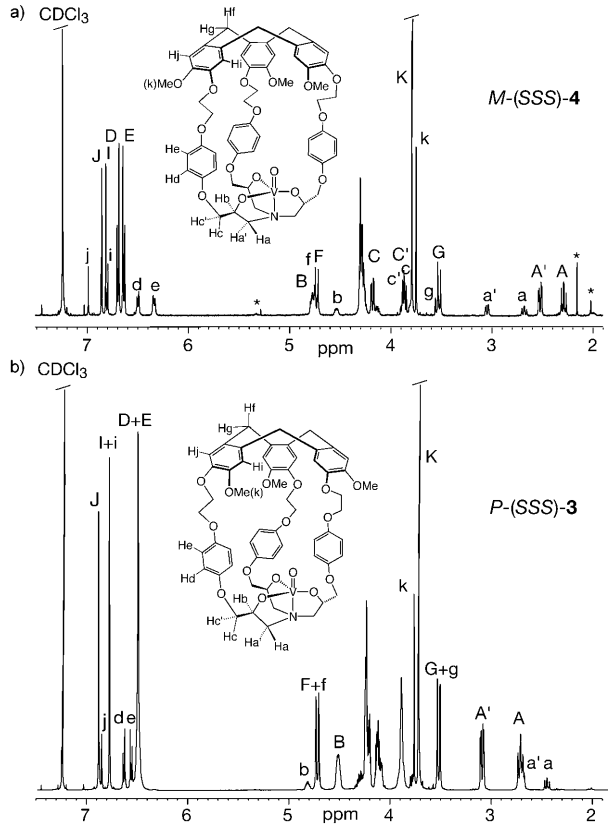

Figure 1. ^{1}H NMR spectra (500 MHz, 298 K) of diastereomers a) (*M*)-(*S*,*S*,*S*)-**4** and b) (*P*)-(*S*,*S*,*S*)-**3** in $CDCl_3$ solution. Upper-case and lower-case letters denote the major and minor species, respectively (*: impurities from the solvent).

sets of related signals indicative of the presence in solution of two compounds with C_3 symmetry. The ^{1}H NMR spectrum of (*M*)-(*S*,*S*,*S*)-**4** in $CDCl_3$, for instance, displays two pairs of singlets for the CTV units, two singlets for the OCH_3 groups, and two characteristic AB systems for the Ar-CH_2 bridges. Similarly, two sets of signals are observed for the protons assigned to the atrane moieties (Figure 1a). Integration of the NMR signals gives a 1:0.35 molar ratio for the two species at 298 K. We therefore assumed that two C_3-symmetric hemicryptophane complexes are present in solution. The same conclusion can be drawn from the ^{1}H NMR spectrum of (*P*)-(*S*,*S*,*S*)-**3** in $CDCl_3$, which revealed the presence of two hemicryptophane complexes with C_3 symmetry in a 1:0.17 ratio (Figure 1b).

A further insight into the natures of the two species was obtained from the ^{51}V NMR spectrum of (*M*)-(*S*,*S*,*S*)-**4** in $CDCl_3$. Two signals were detected in the range typical of five-coordinate vanadium complexes with an O_4N donor set ($\delta = -382.5$ and -397.1 ppm),[13] suggesting the presence of two isomers in solution (Figure 2a). These signals could thus be attributed, with reference to the data reported in the literature, to two different trigonal bipyramidal vanadium complexes with N-amine *trans* to the oxo group.[14] Integration of the signals in the ^{51}V NMR spectrum of (*M*)-(*S*,*S*,*S*)-**4** confirmed the 1:0.35 ratio observed for the two species in the ^{1}H NMR spectra. A similar, but less well-resolved, ^{51}V NMR spectrum was observed with (*P*)-(*S*,*S*,*S*)-**3** (Figure 2b). This is in good agreement with the presence of two C_3-symmetric hemicryptophane oxidovanadium(V) complexes in solution. These results definitively rule out the monomer/dimer hypothesis, because the C_3 symmetry would be lost in that case. Additionally, variation in concentration did not change the relative intensities of both species. Moreover, alkoxidovanadium compounds tend to associate into dimers/oligomers through alkoxo bridges and additional ^{51}V NMR signals should therefore have been observed in the higher-field region.[12,15]

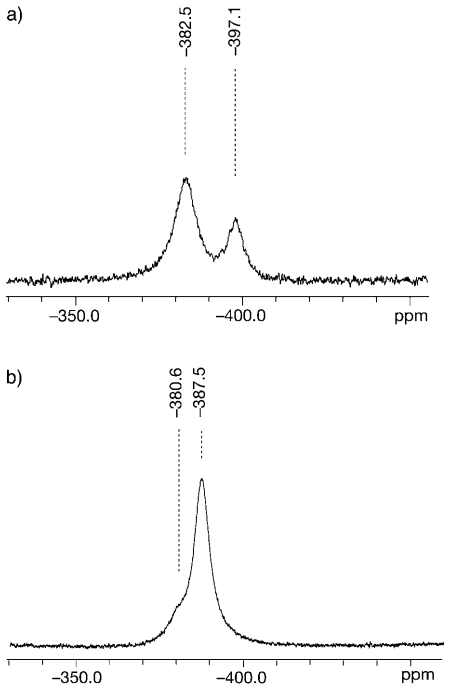

Figure 2. ^{51}V NMR spectra (131.4 MHz, 298 K) of a) (*M*)-(*S*,*S*,*S*)-**4** and b) (*P*)-(*S*,*S*,*S*)-**3** in $CDCl_3$ solution.

Equilibrium between two diastereomers accounts for such a NMR behavior: the conformational mobility of the three five-menbered rings of the atrane structure is probably reduced by the rigidity of the CTV moiety, and the propeller arrangement around the N−V bond leads to the formation of Λ and Δ diastereomers. Therefore, on the NMR time scale, the low rate for the interconversion results in the observation of the two diastereomeric complexes (*M*)-(*S*,*S*,*S*-Λ)-**4** and (*M*)-(*S*,*S*,*S*-Δ)-**4**, which are responsible for the two sets of signals observed in the NMR spectra. Similarly, a mixture of two diastereomers (*P*)-(*S*,*S*,*S*-Λ)-**3**, (*P*)-(*S*,*S*,*S*-Δ)-**3** exists in solution since two sets of NMR signals are also observed.

X-ray diffraction analysis: Single crystals of (*P*)-(*S*,*S*,*S*)-**3** suitable for X-ray analysis were obtained from a dichloromethane/toluene solution by slow evaporation. A represen-

tation of the structure is shown in Figure 3 and key interatomic distances and angles around the vanadium atom are summarized in Table 1. The molecule adopts a compact

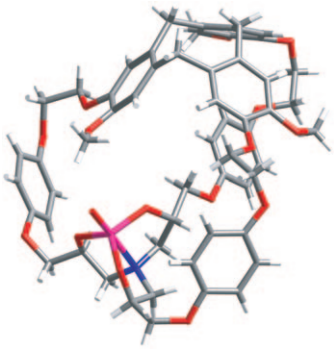

Figure 3. X-ray molecular structure of (*P*)-(*S*,*S*,*S*-Λ)-**3** showing the chiral arrangement of the vanatrane moiety.

structure with the CTV cavity occupied by one of the linkers, so that the atrane moiety is pushed outwards. This is an unexpected form of the molecular host, which generally exists as a solvate with an encapsulated guest solvent inside the molecular cavity.

Table 1. Selected interatomic distances [Å] and angles [°] extracted from X-ray analysis of (*P*)-(*S*,*S*,*S*-Λ)-**3** and DFT-optimized parameters of (*P*)-(*S*,*S*,*S*-Λ)-**3** and (*P*)-(*S*,*S*,*S*-Δ)-**3**.

	(*P*)-(*S*,*S*,*S*-Λ)-**3** X-ray data	(*P*)-(*S*,*S*,*S*-Λ)-**3** calcd	(*P*)-(*S*,*S*,*S*-Δ)-**3** calcd
V–N	2.310	2.50	1.99
V=O	1.592	1.61	1.70
V–O	1.791–1.805	1.80	1.94
O=V–N	178.1	180	180
O=V–O	100.1–102.5	103	93
O–V–O	115.6–117.3	114	120
N–V–O	78.3–79.1	76	87
V–N–C	104.9–106.1	104	105
C–N–C	112.8–114.1[a]	115[b]	114[c]

[a] Σ(C–N–C angles) = 339.74°. [b] 345°. [c] 342°.

Two types of structures for hemicryptophanes and cryptophanes are known. On one hand they are easily able to encapsulate guests such as chloroform or toluene in their cavities.[2,3,4d] On the other hand, inverted or imploded cryptophanes, with characteristic NMR signals for molecules with lower symmetry, have been described in the literature.[2e,16] Clearly, this structure does not account for the solution behavior. Indeed, the ^{1}H NMR spectrum of (*P*)-(*S*,*S*,*S*)-**3** shows that both diastereomeric compounds in equilibrium possess C_3 symmetrical axes. Moreover, strong chemical shift variations should be observed if the X-ray structure reflected the conformation of one of the species in solution.[16a] More interestingly, this structure reveals that only one diastereomer—(*P*)-(*S*,*S*,*S*-Λ)-**3**—crystallizes from the solution (space group *I*4 (79)). This corresponds to the anticlockwise propeller arrangement for the atrane rings when viewed down the N–V–O axis (Figure 4). This fits with a release of

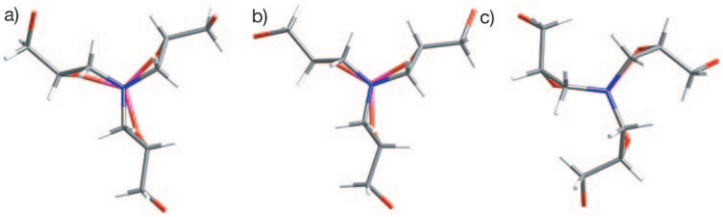

Figure 4. Conformation of the atrane moiety in a) the X-ray structure of (*P*)-(*S*,*S*,*S*-Λ)-**3**, and in the b) Λ and c) Δ DFT-optimized structures (viewed along the N–V–O axis, with N at the top). Atom color: C) gray, N) blue, O) red, V) magenta.

the strains, induced by the cage structure, as the linker substituents that bind the CTV unit to the atrane five-membered rings adopt the less hindered pseudoequatorial orientation.

Crystals of (*P*)-(*S*,*S*,*S*)-**3** dissolved in $CDCl_3$ showed only one set of signals in the ^{1}H NMR spectrum, consistently with the structure of one diastereomer with C_3 symmetry (Figure 5). This diastereomer corresponds to the major compound observed in Figure 1b, and slowly equilibrates at 298 K to give the 1:0.17 ratio for the two diastereomers (*P*)-(*S*,*S*,*S*-Λ)-**3** and (*P*)-(*S*,*S*,*S*-Δ)-**3**. The Λ form is thus predominant both in the analyzed crystal and in chloroform solution. The substituents on the atrane structure preferentially adopt the pseudoequatorial orientation.

Molecular modeling: The Λ and Δ forms of the atrane moiety in the (*P*)-(*S*,*S*,*S*)-**3** and (*M*)-(*S*,*S*,*S*)-**4** complexes had been characterized by NMR in solution and the X-ray analysis of (*P*)-(*S*,*S*,*S*-Λ)-**3** had revealed an unexpected hemicryptophane structure without any well-defined free molecular

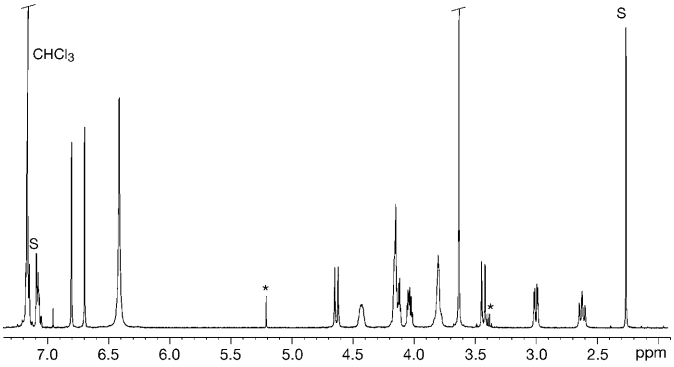

Figure 5. ^{1}H NMR spectrum (500 MHz, 298 K) of crystalline (*P*)-(*S*,*S*,*S*-Λ)-**3** immediately after dissolution in $CDCl_3$ (S: toluene solvent from the crystal; *: solvent impurities).

cavity. In the preferred conformation (the Λ form), the linkers adopt pseudoequatorial orientations that release steric strains around the atrane unit. We thus became interested in investigating the relative stabilities of the Λ and the Δ forms further and addressed this question by means of density functional theory (DFT) calculations. In order to quantify the relative energies of the different diastereomers, complementary calculations were performed. Full geometry optimizations were first carried out on the *P* diastereomeric pair. In view of the system's size, this initial procedure is desirable to check the validity of the DFT geometry optimization. Whatever the solvent, the experimental data favor the major (*P*)-(*S*,*S*,*S*-Λ) species, so the gas-phase theoretical calculations should confirm this trend. The structures of the two diastereomers (*P*)-(*S*,*S*,*S*-Λ)-**3** and (*P*)-(*S*,*S*,*S*-Δ)-**3** were optimized with respect to all geometrical parameters by a BP86/DFT approach, leading to global minima (Figure 6).

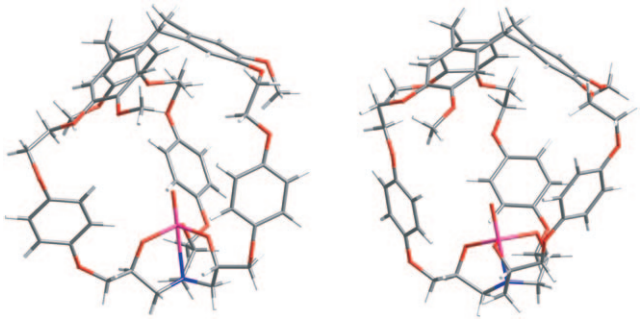

Figure 6. DFT-optimized structures for the (*P*)-(*S*,*S*,*S*-Λ)-**3** (left) and (*P*)-(*S*,*S*,*S*-Δ)-**3** (right) complexes.

As can be seen in Table 1, the optimized bond lengths and valence angles are in very good agreement with the X-ray data. The two species each present a well-defined molecular cavity with a propeller-like arrangement of the vanadium atrane structure. The (*P*)-(*S*,*S*,*S*-Λ)-**3** diastereomer is energetically favored over the (*P*)-(*S*,*S*,*S*-Δ)-**3** one by 34 kJ mol^{-1}. This result suggests that the helical structure of the atrane moiety is favored for the pseudoequatorial orientations of the linkers that connect the CTV unit (Figure 4). The Λ propeller-like conformation is thus more stable than the Δ propeller, and the diastereomer (*P*)-(*S*,*S*,*S*-Λ)-**3** predominates at equilibrium.

Because attempts to obtain crystals of (*M*)-(*S*,*S*,*S*)-**4** suitable for X-ray analysis failed, a similar computational approach was used to analyze the *M* diastereomeric pair. Although DFT calculations may suffer from overestimation of interatomic distances, comparison between the reference *P* isomers and the *M* ones should provide further insights into the relative energies of the *M* diastereomers. The results obtained for the *M* diastereomeric pair (Figure 7), are similar to those previously obtained for (*P*)-(*S*,*S*,*S*)-**3**: the propeller-like vanatrane with pseudoequatorial substituents is the more stable conformation (favored over the pseudoaxial by 25 kJ mol^{-1}). The major and minor sets of signals in the

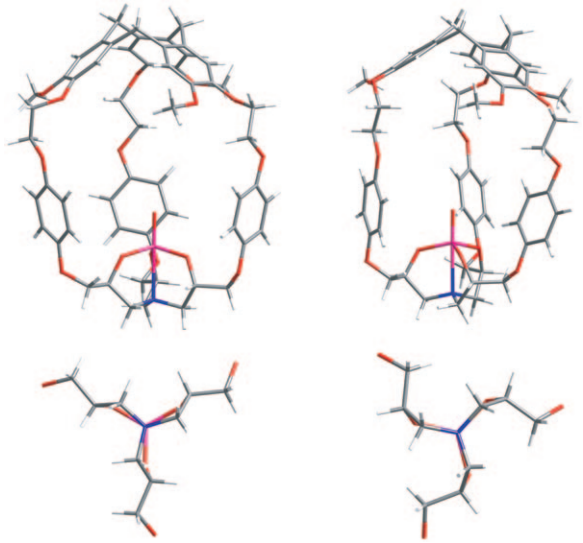

Figure 7. DFT-optimized structures for the (*M*)-(*S*,*S*,*S*-Λ)-**4** (left) and (*M*)-(*S*,*S*,*S*-Δ)-**4** (right) complexes, and the conformations of their corresponding atrane moieties viewed along the N–V–O axes, with N at the top. Atom color: C) gray, N) blue, O) red, V) magenta.

NMR spectrum of (*M*)-(*S*,*S*,*S*)-**4** can therefore be attributed to the diastereomers (*M*)-(*S*,*S*,*S*-Λ)-**4** and (*M*)-(*S*,*S*,*S*-Δ)-**4**, respectively.

NMR spectroscopy studies: The Λ⇄Δ equilibrium for the diastereomers (*P*)-(*S*,*S*,*S*)-**3** and (*M*)-(*S*,*S*,*S*)-**4** has been studied in solution by NMR spectroscopy. The Λ and Δ forms of both diastereomers are in equilibrium, with the Λ:Δ ratio varying only slightly with the temperature. In $CDCl_3$ solution, for instance, the (*M*)-(*S*,*S*,*S*-Λ)-**4**/(*M*)-(*S*,*S*,*S*-Δ)-**4** and (*P*)-(*S*,*S*,*S*-Λ)-**3**/(*P*)-(*S*,*S*,*S*-Δ)-**3** ratios shift from 1:0.29 and 1:0.16 at 278 K to 1:0.42 and 1:0.17 at 333 K, respectively. However, no coalescence was reached up to 403 K (in DMSO), suggesting slow interconversion rates for the Λ and Δ forms of (*P*)-(*S*,*S*,*S*)-**3** and (*M*)-(*S*,*S*,*S*)-**4** over the investigated temperature range. From these experiments, we estimated the thermodynamic parameters for both equilibrium reactions with enthalpy values $\Delta H^\circ = -1.2$ and -5.2 kJ mol^{-1}, and entropy values $\Delta S^\circ = 10.8$ and -8.3 J mol^{-1} K^{-1} for (*P*)-(*S*,*S*,*S*)-**3** and (*M*)-(*S*,*S*,*S*)-**4**, respectively; see the Supporting Information. In contrast, a change in solvent causes dramatic modification of the Λ:Δ ratios for the two species (Figure 8). We may note that the Λ form is still the major one whatever the complex or the solvent used. The diastereomeric excess for (*P*)-(*S*,*S*,*S*)-**3** shifts from 11% in DMSO to 94% in benzene. A strong but opposite solvent effect was also observed with (*M*)-(*S*,*S*,*S*)-**4**, with the diastereomeric excess shifting from 0% in benzene to 92% in DMSO (Table 2 and Figure 8). These results show that the clockwise or anticlockwise orientations of the propeller-like atrane structures are largely governed by the solvent both in diastereomer (*P*)-(*S*,*S*,*S*)-**3** and in diastereomer (*M*)-(*S*,*S*,*S*)-**4**. However, the explanation for that behavior remains unclear, although the configurations of the CTV units,

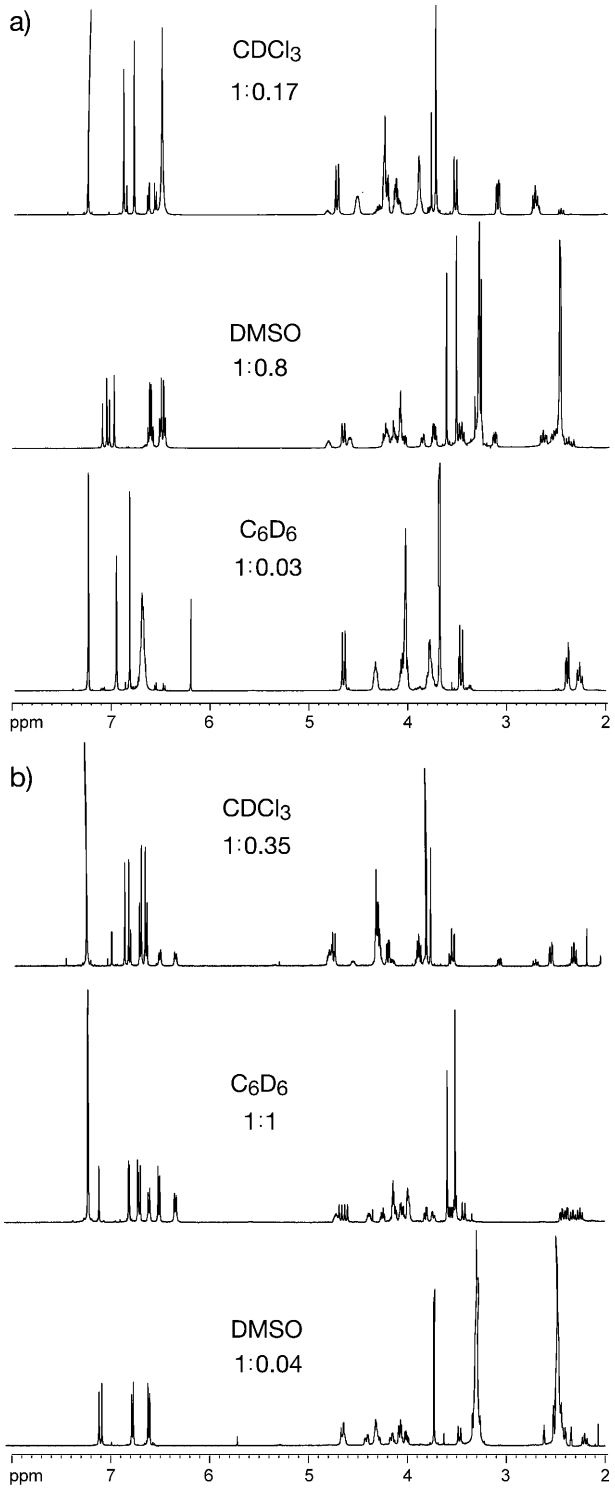

Figure 8. ^{1}H NMR spectra (500 MHz, 298 K) showing the solvent effect on the clockwise vs. anticlockwise orientations of the propeller-like atrane moieties in the diastereomeric hemicryptophanes a) (*P*)-(*S*,*S*,*S*)-**3** and b) (*M*)-(*S*,*S*,*S*)-**4**.

the polarity of the solvent, and the inclusion of a solvent guest should be considered.

The free energies of activation ($\Delta G^{\neq}$) for stereoconversion were determined from NMR experiments (Table 3).

Table 2. Diastereomeric excesses (*de*s) for (*P*)-(*S*,*S*,*S*)-**3** and (*M*)-(*S*,*S*,*S*)-**4** complexes in different solvents ($T=298$ K).

Complex	C_6D_6 [%]	$CDCl_3$ [%]	DMSO [%]
(*P*)-(*S*,*S*,*S*)-**3**	94	70	11
(*M*)-(*S*,*S*,*S*)-**4**	0	48	92

The diastereomerically pure sample of (*P*)-(*S*,*S*,*S*-Λ)-**3** (crystals) and a 1:1 mixture of (*M*)-(*S*,*S*,*S*-Λ)-**4** and (*M*)-(*S*,*S*,*S*-Δ)-**4** (from evaporation of a benzene solution) were separately dissolved in $CDCl_3$, and equilibration was monitored by ^{1}H NMR spectroscopy. The activation parameters were calculated from the $\Delta G^{\neq}$ values obtained at different temperatures (Table 3).

Table 3. Activation parameters for the stereoconversion barriers in (*P*)-(*S*,*S*,*S*)-**3** and (*M*)-(*S*,*S*,*S*)-**4**.

Complex	$\Delta G^{\neq}$ [kJ mol^{-1}][a]	$\Delta H^{\neq}$ [kJ mol^{-1}]	$\Delta S^{\neq}$ [J mol^{-1} K^{-1}]
(*P*)-(*S*,*S*,*S*)-**3**	103.7	30.8	−243
(*M*)-(*S*,*S*,*S*)-**4**	94.0	13.3	−272

[a] $T=298$ K.

The mechanism for the ring flipping could be either a stepwise or a concerted one. Supporting evidence for a concerted mechanism was provided by the large negative values of the activation entropies: $\Delta S^{\neq}=-243$ and -272 J mol^{-1} K^{-1} for (*P*)-(*S*,*S*,*S*)-**3** and (*M*)-(*S*,*S*,*S*)-**4**, respectively. This would be expected if the transition state for the stereoconversion process were more symmetrical than both diastereomers, as could be accomplished if, for instance, (*P*)-(*S*,*S*,*S*-Λ)-**3** or (*M*)-(*S*,*S*,*S*-Λ)-**4** were to adopt the transition state depicted in Scheme 3, to give (*P*)-(*S*,*S*,*S*-Δ)-**3** and (*M*)-(*S*,*S*,*S*-Δ)-**4**, respectively. The $\Delta G^{\neq}$ values of 103.7 and 94.0 kJ mol^{-1} obtained for (*P*)-(*S*,*S*,*S*)-**3** and (*M*)-(*S*,*S*,*S*)-**4**, respectively, are higher than all those previously reported for atrane derivatives. To the best of our knowledge, the highest value reported in the literature is for an azaboratrane derivative ($\Delta G^{\neq}=74$ kJ mol^{-1}).[10] The rigidity of the hemicryptophane complexes undoubtedly arises from steric hindrance due to the three arms linking the CTV cap.

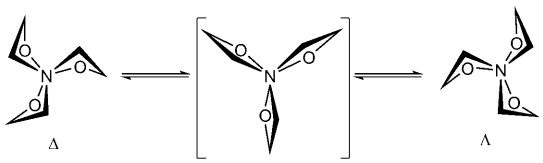

Scheme 3. Expected transition structure geometry for the clockwise/anticlockwise interconversion mechanism of the propeller-like vanatrane moieties (viewed along the N–V–O axis, with N at the top).

It may be noted that the Λ/Δ exchange involves clockwise or anticlockwise motion of the vanatrane moiety. Consequently, dissolution of a 1:0.35 (*M*)-(*S*,*S*,*S*-Λ)-**4**/(*M*)-(*S*,*S*,*S*-Δ)-**4** mixture in benzene leads to a preferential clockwise ro-

tational motion (i.e., the Λ:Δ ratio decreases from 1:0.35 to 1:1), whereas dissolution in DMSO leads to a preferential anticlockwise rotational motion (i.e., the Λ:Δ ratio increases from 1:0.35 to 1:0.04). In the same way, dissolution of a 1:0.17 (*P*)-(*S*,*S*,*S*-Λ)-**3**/(*P*)-(*S*,*S*,*S*-Δ)-**3** mixture in DMSO leads to a preferential clockwise rotational motion (i.e., the Λ:Δ ratio decreases from 1:0.17 to 1:0.8), whereas dissolution in benzene leads to a preferential anticlockwise rotational motion (i.e., the Λ:Δ ratio increases from 1:0.17 to 1:0.03). Solvents can therefore monitor the helical chirality of the vanatrane derivatives.

Conclusions

We have shown here that the hemicryptophane oxidovanadium(V) complexes (*P*)-(*S*,*S*,*S*)-**3** and (*M*)-(*S*,*S*,*S*)-**4** adopt different conformations due to the atrane structure of the vanadyl moiety. The propeller-like vanatrane structure leads to the (*P*)-(*S*,*S*,*S*-Λ)-**3**/(*P*)-(*S*,*S*,*S*-Δ)-**3** and (*M*)-(*S*,*S*,*S*-Λ)-**4**/(*M*)-(*S*,*S*,*S*-Δ)-**4** diastereomers, respectively. The Λ⇄Δ exchange process is slow on the NMR timescale, allowing the observation of both Λ and Δ forms for each complex in solution. Only the (*P*)-(*S*,*S*,*S*-Λ)-**3** isomer crystallizes from the (*P*)-(*S*,*S*,*S*-Λ)-**3**/(*P*)-(*S*,*S*,*S*-Δ)-**3** CH_2Cl_2/toluene solution, and shows an unexpected flattened structure with the Λ conformation of the vanatrane moiety. Optimized structures obtained from DFT calculations confirm that the (*P*)-(*S*,*S*,*S*-Λ)-**3** diastereomer is the more stable, consistently with the experimental data. Similarly, our calculations show that the diastereomer (*M*)-(*S*,*S*,*S*-Λ)-**4** is preferred. In solution, the Λ⇄Δ interconversion is most likely due to a concerted mechanism rather than to a stepwise process and likely proceeds via a pseudo C_{3h}-symmetric transition state of the vanatrane structure. The energy barriers for the Λ⇄Δ equilibria observed in the complexes (*P*)-(*S*,*S*,*S*)-**3** and (*M*)-(*S*,*S*,*S*)-**4** are higher than those reported for other atrane derivatives. The solvent was shown to affect the Λ:Δ ratio strongly and also to control the preferential direction of the clockwise or anticlockwise rotational motion. The helical chirality (i.e., the Δ or Λ configuration) of the atrane moiety can thus be strongly modified simply by changing the solvent. This unusual chirality switch, controlled by an external factor, remains a challenge for information storage based on stereochemical changes. Moreover, the hemicryptophane complexes model specific features of vanadate-dependent haloperoxydases, such as the trigonal-bipyramidal O_4N coordination of oxidovanadium(V) and the chiral environment of the active center.[17] These complexes are very promising because supramolecular asymmetric catalytic properties can be anticipated. Such studies are currently in progress.

Experimental Section

Materials and instrumentation: ^1H and ^{51}V NMR spectra were recorded at 500.1 MHz and 131.54 MHz, respectively with a Brucker DPX 500 spectrometer and are reported relative to the residual protonated solvent signals (^1H) or to external $VOCl_3$ (^{51}V). $VO(iPrO)_3$ (Aldrich) was used as obtained. The hemicryptophanes (*P*)-(*S*,*S*,*S*)-**1** and (*M*)-(*S*,*S*,*S*)-**2** and complex (*P*)-(*S*,*S*,*S*)-**3** were prepared as previously described.[6]

Computational method: Ab initio evaluations were performed with the aid of the Gaussian 03 package within a restricted DFT framework. A combination of unrestricted BP86 functional and triple-zeta 6–311G all-electron basis sets has proven to be very satisfactory for geometry optimizations.[18,19] We used the hybrid B3LYP functional to check that our results do not suffer from the arbitrariness of the exchange correlation functional.

Oxidovanadium(V) complexes (*P*)-(*S*,*S*,*S*)-3 and (*M*)-(*S*,*S*,*S*)-4: These complexes were prepared by the synthetic scheme reported previously. Typically, oxidovanadium(V) triisopropoxide (14.4 μL, 15.6 mg, 1 equiv) was added by microsyringe to a solution of (*M*)-(*S*,*S*,*S*)-**2** (64 mg, 6.38×10^{-5} mol) in $CHCl_3$ (4 mL). After stirring at room temperature for 40 min, the solution was concentrated, washed with diethyl ether, and dried under vacuum.

Complex (*P*)-(*S*,*S*,*S*)-3: ^1H NMR (500 MHz, $CDCl_3$; M: major compound; m: minor compound, M/m = 1:0.18): δ = 6.88 (s, 3H; Hi,M), 6.85 (s, 3H; Hi,m), 6.77 (s, 3HM+3Hm; Hh,M, Hh,m), 6.63 (d, J = 9.15 Hz, 6H; Hd,m), 6.56 (d, J = 9.15 Hz, 6H; He,m), 6.49 (s, 12H; Hd,M, He,M), 4.84–4.78 (m, 3H; Hb,m), 4.71 (d, J = 13.55 Hz, 3HM+3Hm; HF,M, HF,m), 4.54–4.46 (m, 3H; Hb,M), 4.34–4.04 (m, 12HM+15Hm; Hl,M, Ho,M, Hl,m, Ho,m and Hc,m), 3.88 (br s, 6H; Hc,M, Hc′,M), 3.79–3.75 (m, 3H; Hc′,m), 3.75 (s, 9H; Hk,m), 3.71 (s, 9H; Hk,M), 3.51 (d, J = 13.55 Hz, 3HM+3Hm; Hj,m and Hj,M), 3.08 (dd, J = 13.0 and 4.0 Hz, 3H; Ha,M), 2.70 (t, J = 11.95 Hz, 3H; Ha′M), 2.69–2.65 (m, 3H; Ha,m), 2.43 ppm (t, J = 11.85 Hz, 3H; Ha′,m).

Complex (*M*)-(*S*,*S*,*S*)-4: ^1H NMR (500 MHz, $CDCl_3$; M: major compound, m: minor compound, M/m = 1:0.35): δ = 6.99 (s, 3H; Hi,m), 6.86 (s, 3H; Hi,M), 6.82 (s, 3H; Hh,M), 6.80 (s, 3H; Hh,m), 6.70 (d, J = 9.2 Hz, 6H; Hd,M), 6.64 (d, J = 9.2 Hz, 6H; He,M), 6.50 (d, J = 8.9 Hz, 6H; Hd,m), 6.34 (d, J = 8.9 Hz, 6H; Hd,m), 4.80–4.73 (m, 3H; Hb,M), 4.74 (d, J = 13.55 Hz, 3H; Hf,m), 4.74 (d, J = 13.55 Hz, 3H; Hf,m), 4.73 (d, J = 13.8 Hz, 3H; Hf,M), 4.58–4.50 (m, 3H; Hb,m), 4.32–4.11 (m, 12HM+12Hm; Hl,M, Ho,M, Hl,m and Ho,m), 4.18 (dd, J = 11.95 and 3.8 Hz, 3H; Hc,M), 3.91–3.85 (m, 3HM+6Hm; Hc′,M, Hc,m and Hc′,m), 3.80 (s, 9H; Hk,M), 3.75 (s, 9H; Hk,m), 3.55 (d, J = 13.55 Hz, 3H; Hj,m), 3.52 (d, J = 13.8 Hz, 3H; Hj,M), 3.05 (dd, J = 13.0, 4.2 Hz, 3H; Ha,m), 2.68 (t, J = 12.1 Hz, 3H; Ha′,m), 2.51 (dd, J = 12.9, 3.7 Hz, 3H; Ha,M), 2.28 ppm (t, J = 11.15 Hz, 3H; Ha′M).

X-ray crystallography: X-ray diffraction data for (*P*)-(*S*,*S*,*S*)-**3**·1.25 toluene were collected at low temperatures with use of an oil-coated shock-cooled crystal and a Bruker-AXS APEX2 diffractometer with MoKα radiation (λ = 0.71073 Å). The structures were solved by direct methods (SHELXS-97)[20] and all non-hydrogen atoms were refined anisotropically by the least-squares method on F^2.[21]

Crystal data for (P)-(S,S,S)-3·1.25 toluene: $C_{65.75}H_{70}NO_{16}V$, M = 1181.17, tetragonal, $I4$, $a=b$ = 28.8139(8) Å, c = 15.5279(8) Å, V = 12891.9(8) Å^3, Z = 8, T = 173(2) K, 73778 reflections (8261 independent, R_{int} = 0.0822), largest electron density residue: 0.671 e Å^{-3}, $R1$ (for $I>2\sigma(I)$) = 0.0503 and $wR2$ = 0.1404 (all data) with $R1=\Sigma||F_o|-|F_c||/\Sigma|F_o|$ and $wR2=(\Sigma w(F_o^2-F_c^2)^2/\Sigma w(F_o^2)^2)^{0.5}$. The absolute structure parameter refined to −0.05(3).[22] Data for all structures were collected.

CCDC 739478 contains the supplementary crystallographic data for this paper. These data can be obtained free of charge from The Cambridge Crystallographic Data Centre via www.ccdc.cam.ac.uk/data_request/cif

Acknowledgements

Mr. J.-C. Mulatier is gratefully acknowledged for skilful experimental contribution. We thank Dr. L. Guy for helpful discussion.

[1] a) A. J. Kirby, *Angew. Chem.* **1996**, *108*, 770–790; *Angew. Chem. Int. Ed. Engl.* **1996**, *35*, 707–724; b) J. K. M. Sanders, *Chem. Eur. J.* **1998**, *4*, 1378–1383; c) J.-M. Lehn, *Rep. Prog. Phy.* **2004**, *67*, 245–249.

[2] a) L. Garel, J.-P. Dutasta, A. Collet, *Angew. Chem.* **1993**, *105*, 1249–1251; *Angew. Chem. Int. Ed. Engl.* **1993**, *32*, 1169–1171; b) A. Collet, J.-P. Dutasta, B. Lozach, J. Canceill, *Top. Curr. Chem.* **1993**, *165*, 103–129; c) L. Garel, B. Lozach, J.-P. Dutasta, A. Collet, *J. Am. Chem. Soc.* **1993**, *115*, 11652–11653; d) H. A. Fogarty, P. Berthault, T. Brotin, G. Huber, H. Desvaux, J.-P. Dutasta, *J. Am. Chem. Soc.* **2007**, *129*, 10332–10333; e) T. Brotin, J.-P. Dutasta, *Chem. Rev.* **2009**, *109*, 88–130.

[3] a) J. Canceill, L. Lacombe, A. Collet, *J. Am. Chem. Soc.* **1985**, *107*, 6993–6996; b) J. Costante-Crassous, T. J. Marrone, J. M. Briggs, J. A. McGammon, A. Collet, *J. Am. Chem. Soc.* **1997**, *119*, 3818–3823; c) J. Crassous, S. Hediger, *J. Phys. Chem. A* **2003**, *107*, 10233–10240.

[4] a) J. Canceill, A. Collet, J. Gabard, F. Kotzyba-Hibert, J.-M. Lehn, *Helv. Chim. Acta* **1982**, *65*, 1894–1897; b) J. W. H. Smeets, H. K. A. C. Coolen, J. W. Zwikker, R. J. M. Nolte, *Recl. Trav. Chim. Pays-Bas* **1989**, *108*, 215–218; c) G. Rapenne, J. Crassous, A. Collet, L. Echegoyen, F. Diederich, *Chem. Commun.* **1999**, 1121–1122; d) I. Gosse, J.-P. Dutasta, M. Perrin, A. Thozet, *New J. Chem.* **1999**, *23*, 545–548.

[5] A. Collet, in *Comprehensive Supramolecular Chemistry, Vol. 2* (Ed.: F. Vögtle), Pergamon Press, New York, **1996**, pp. 325–365.

[6] A. Gautier, J.-C. Mulatier, J. Crassous, J-P. Dutasta, *Org. Lett.* **2005**, *7*, 1207–1210.

[7] a) J. G. Verkade, *Acc. Chem. Res.* **1993**, *26*, 483–489; b) J. G. Verkade, *Coord. Chem. Rev.* **1994**, *137*, 233–295; c) R. R. Schrock, *Acc. Chem. Res.* **1997**, *30*, 9–16.

[8] M. Tasaka, M. Hirotsu, M. Kojima, *Inorg. Chem.* **1996**, *35*, 6981–6986.

[9] E. M. Evgeniou, S. A. Pergantis, E. Leontidis, A. D. Keramidas, *Inorg. Chem.* **2005**, *44*, 7511–7522.

[10] J. Pinkas, B. Gaul, J. G. Verkade, *J. Am. Chem. Soc.* **1993**, *115*, 3925–3931.

[11] a) A. Chandrasekaran, R. O. Day, R. R. Holmes, *J. Am. Chem. Soc.* **2000**, *122*, 1066–1072; b) N. V. Timosheva, A. Chandrasekaran, R. O. Day, R. R. Holmes, *Organometallics* **2001**, *20*, 2331–2337.

[12] G. Santoni, G. Licini, D. Rehder, *Chem. Eur. J.* **2003**, *9*, 4700–4708.

[13] D. Rehder, C. Weidmann, A. Duch, W. Priebsch, *Inorg. Chem.* **1988**, *27*, 584–587.

[14] D. C. Crans, C. Haojiang, O. P. Anderson, M. M. Miller, *J. Am. Chem. Soc.* **1993**, *115*, 6769–6776.

[15] a) W. Priebsch, D. Rehder, *Inorg. Chem.* **1990**, *29*, 3013–3019; b) F. Hillerns, F. Olberich, U. Behrens, D. Rehder, *Angew. Chem.* **1992**, *104*, 479–480; *Angew. Chem. Int. Ed. Engl.* **1992**, *31*, 447–448; c) O. W. Howarth, J. R. Trainor, *Inorg. Chem. Acta* **1987**, *127*, L27; d) D. C. Crans, F. Jiang, J. Chen, O. P. Anderson, M. M. Miller, *Inorg. Chem.* **1997**, *36*, 1038–1047.

[16] a) G. Huber, T. Brotin, L. Dubois, H. Desvaux, J.-P. Dutasta, P. Berthault, *J. Am. Chem. Soc.* **2006**, *128*, 6239–6246; b) S. T. Mough, J. C. Goeltz, K. T. Holman, *Angew. Chem.* **2004**, *116*, 5749–5753; *Angew. Chem. Int. Ed.* **2004**, *43*, 5631–5635.

[17] a) A. Messerschmidt, R. Wever, *Proc. Natl. Acad. Sci. USA* **1996**, *93*, 392–396; b) M. Weyand, H. J. Hecht, M. Kiess, M. F. Liaud, H. Vilter, D. Schomburg, *J. Mol. Biol.* **1999**, *293*, 595–611; c) M. I. Isupov, A. R. Dalby, A. A. Brindley, Y. Izumi, T. Tanabe, G. N. Murshudov, J. A. Littlechlid, *J. Mol. Biol.* **2000**, *299*, 1035–1049.

[18] Gaussian 03, M. J. Frisch, G. W. Trucks, H. B. Schlegel, G. E., Scuseria, M. A. Robb, J. R. Cheeseman, G. Scalmani, V. Barone, B. Mennucci, G. A. Petersson, H. Nakatsuji, M. Caricato, X. Li, H. P. Hratchian, A. F. Izmaylov, J. Bloino, G. Zheng, J. L. Sonnenberg, M. Hada, M. Ehara, K. Toyota, R. Fukuda, J. Hasegawa, M. Ishida, T. Nakajima, Y. Honda, O. Kitao, H. Nakai, T. Vreven, J. A. Montgomery, Jr., J. E. Peralta, F. Ogliaro, M. Bearpark, J. J. Heyd, E. Brothers, K. N. Kudin, V. N. Staroverov, R. Kobayashi, J. Normand, K. Raghavachari, A. Rendell, J. C. Burant, S. S. Iyengar, J. Tomasi, M. Cossi, N. Rega, J. M. Millam, M. Klene, J. E. Knox, J. B. Cross, V. Bakken, C. Adamo, J. Jaramillo, R. Gomperts, R. E. Stratmann, O. Yazyev, A. J. Austin, R. Cammi, C. Pomelli, J. W. Ochterski, R. L. Martin, K. Morokuma, V. G. Zakrzewski, G. A. Voth, P. Salvador, J. J. Dannenberg, S. Dapprich, A. D. Daniels, O. Farkas, J. B. Foresman, J. V. Ortiz, J. Cioslowski, D. J. Fox, Gaussian, Inc., Wallingford CT, **2009**.

[19] a) C. H. Chang, A. J. Boone, R. J. Bartlett, N. G. J. Richards, *Inorg. Chem.* **2004**, *43*, 458–472; b) V. Robert, G. Lemercier, *J. Am. Chem. Soc.* **2006**, *128*, 1183–1187.

[20] G. M. Sheldrick, *Acta Crystallogr. Sect. A* **1990**, *46*, 467–473.

[21] SHELXL-97, Program for Crystal Structure Refinement, G. M. Sheldrick, University of Göttingen, Göttingen, **1997**.

[22] H. D. Flack, *Acta Crystallogr. Sect. A* **1983**, *39*, 876–881.

Received: July 16, 2009
Published online: November 13, 2009

